Electrical Power and Energy Systems 109 (2019) 332–342

Contents lists available at ScienceDirect

Electrical Power and Energy Systems

journal homepage: www.elsevier.com/locate/ijepes

Proactive management of distribution grids with chance-constrained linearized AC OPF

Tiago Soares*, Ricardo J. Bessa

INESC Technology and Science (INESC TEC), 4200-465 Porto, Portugal

ARTICLE INFO

Keywords:
Smart grid
Operational planning
Decision-making under uncertainty
Chance-constrained optimization
Renewable energy

ABSTRACT

Distribution system operators (DSO) are currently moving towards active distribution grid management. One goal is the development of tools for operational planning of flexibility from distributed energy resources (DER) in order to solve potential (predicted) congestion and voltage problems. This work proposes an innovative flexibility management function based on stochastic and chance-constrained optimization that copes with forecast uncertainty from renewable energy sources (RES). Furthermore, the model allows the decision-maker to integrate its attitude towards risk by considering a trade-off between operating costs and system reliability. RES forecast uncertainty is modeled through spatial-temporal trajectories or ensembles. An AC-OPF linearization that approximates the actual behavior of the system is included, ensuring complete convexity of the problem. McCormick and big-M relaxation methods are compared to reformulate the chance-constrained optimization problem. The discussion and comparison of the proposed models is carried out through a case study based on actual generation data, where operating costs, system reliability and computer performance are evaluated.

1. Introduction

1.1. Background, methodology and aim

The use of conventional approaches to distribution grid management (also known as reactive approaches) is becoming obsolete as the strong penetration of distributed energy resources (DERs), especially renewable energy sources (RES), introduces new challenges, as well as flexibility, in the operation and management of the distribution grid. Such a paradigm shift in the distribution grid management arises with the concern of dealing with the RES forecast uncertainty that are penetrating the distribution grid and changing the conventional direction of the power flow [1]. Within this scope, traditional grid management methodologies have difficulties in preventing and solving congestion and voltage problems in the distribution grid and can lead to situations were flexibility is not "reserved" to handle local problems. Thus, it becomes crucial to replace or complement such reactive methodologies with new predictive (or proactive) management methodologies that are capable of dealing with the RES forecast uncertainty, and therefore, identify flexibility needs for the next hours that can be later activated to solve congestion and voltage problems [2].

Most of these new methodologies include DER controllability to support grid management. That is, distribution system operators (DSOs) could control generation or flexible loads (to some extent) through pre-contracted flexibility [3]. Still, the DSO will keep the same role, ensuring that congestion, voltage and energy delivery problems are solved with adequate levels of safety, reliability and power quality. In fact, this role can be met to high levels of RES integration by introducing stochastic approaches to the multi-period optimal power flow (OPF). Within this scope, this paper proposes a methodology to support the DSO decisions in the management of the distribution grid under strong penetration of renewable power producers, including stochastic and chance-constrained approaches in a multi-period OPF. The approach enables the DSO to move from reactive distribution management to proactive distribution management, taking advantage of the benefits that this methodology brings to the system reliability.

1.2. Literature review and specific contributions

In the literature, several approaches for distribution grid management proposed different versions of the stochastic OPF problem. A centralized active distribution network under uncertainty using a multi-period backward/forward sweep OPF, and considering single chance-constrained optimization to deal with PV uncertainty was proposed in [4]. In contrast, [5] uses a decentralized stochastic approach based on alternating direction method of multipliers to manage a distribution

* Corresponding author.
E-mail address: tasoares@inesctec.pt (T. Soares).

https://doi.org/10.1016/j.ijepes.2019.02.002
Received 29 October 2018; Received in revised form 24 December 2018; Accepted 1 February 2019
Available online 18 February 2019

Nomenclature

Parameters

ΔP	Power deviation of the scenarios ω
η_{Ch}, η_{Dch}	Charge and discharge efficiency
π	Probability of scenario ω
ang	Angle k of the piecewise linear slopes
B	Imaginary part in admittance matrix
Bus	Number of buses
C	Cost
E_{BatCap}	Maximum capacity of energy storage systems
E_{Min}	Minimum energy in the energy storage system
G	Real part in admittance matrix
M	Large value – Big-M
N	Number of unit resources
Px	Maximum active power of piecewise linear slope
Py	Maximum reactive power of piecewise linear slope
T	Time horizon

Variables

θ	Voltage angle
P	Active power
$\widetilde{P}$	Active power – McCormick relaxation
PWL	Piecewise linearization of cosine function
Q	Reactive power
r	Power flexibility used in the real-time stage
SOC	State of charge of the battery
S	Apparent power
V	Voltage magnitude
V_{sb}	Voltage at slack bus
ΔV	Voltage level activated by the DSO in the transformer
X	Binary variable
Z	Auxiliary variable for absolute function linearization

Subscripts

ω	Index of scenarios
cb	Index of capacitor bank units
CB	Capacitor bank abbreviation
Ch	Storage charge process
Dch	Storage discharge process
dg	Index of distributed generation units
DG	Distributed generation abbreviation
DR	Demand response abbreviation
Flow	Power flow in the line *i,j*
i, *j*	Bus index
k	Index of piecewise linear slopes
l	Index of load consumers
L	Load consumers abbreviation
lv	Index of levels (tap changing) for capacitor banks and transformers
pv	Index of photovoltaic power units
PV	Photovoltaic power abbreviation
st	Index of energy storage system units
ST	Energy storage system abbreviation
su	Index of external supplier units
SU	External supplier abbreviation
t	Time index
trf	Index of transformer units
TRF	Transformer abbreviation
w	Index of wind power units
W	Wind power abbreviation

Superscripts

act	Activation cost of resources in real-time stage
bid_dw	Maximum offer of downward flexibility
bid_up	Maximum offer of upward flexibility
CC	Chance-constrained
cut	Generation curtailment power for distributed generation
dw	Downward flexibility
Max	Maximum limit
Min	Minimum limit
op	Operating point of the power resource
shed	Load shedding
spill	Spillage of renewable energy
Total	Total power of the unit
up	Upward flexibility

grid with PV. However, both models are effective only for distribution grids under radial or weak meshed topology, considering iterative OPF techniques. Many authors use stochastic and chance-constrained approaches to cope with the uncertain RES generation in distribution grid management, whether for frequency or voltage control [4,6–9]. A general stochastic framework for DER (including RES) scheduling at the distribution level is shown in [6]. This approach aims to schedule the energy and reserve of the DER in distribution grids, disregarding the flexibility of RES and the use of static equipment in the distribution grid. In contrast, [4] proposes an active distribution management based on the DER control (such as distributed generation, controllable loads and energy storage systems) and considering an iterative approach of the backward and forward sweep power flow method. Reactive power control is assured by the DER, while static equipment (e.g. capacitor banks) in the distribution network is disregarded. Chance-constrained programming is used to cope with uncertain power production, limiting the probability of insecure operation. Similarly, [7] uses a chance-constrained approach to address and mitigate the risk of variable over voltage, excessive tap cunts, and voltage regulator runaway in the distribution network under photovoltaic penetration. The chance-constraint is applied to limit the bus voltage violation, feeder current and tap changing of the transformer, disregarding flexibility from DER. In contrast, [8] introduces active distribution management directed to voltage and reactive power control using chance-constrained to deal with RES uncertainty. It proposes an iterative process in which the validation of each individual scenario is performed primarily, followed by the chance–constrained approach in case of scenario violation. A chance-constrained approach for optimal power flow in distribution networks is proposed in [9], using the two-point estimate method [10] to determine the probabilistic load flow. Applies chance constraints to state variables constraints instead of active and reactive power balance constraints. These works end up using probabilistic load flow and OPF, which most often results in a distribution of the decision variables, instead of a single set of decision variables (or control set-points). Other works argue that a single feasible distribution management solution for all or a predefined set of scenarios would be the most suitable solution for a DSO [11–13]. However, most of these stochastic/robust-based techniques are generally very hard to converge, and therefore the convexification of nonconvex nonlinearities is required.

In this context, the proposed work describes a two-stage stochastic chance-constrained OPF that integrates RES forecast uncertainty, sharing similar structure and formulation as in the well-known stochastic unit-commitment problem under chance-constrained programming [14–22]. In addition, the work follows a recent trend in the

scientific community where the DSO preventively manages the distribution grid by contracting flexibility from DER ahead of the operating stage [9,23–25]. The problem is narrowed down to cope with the characteristics of the distribution system (all assumptions for the OPF are based on typical distribution network characteristics), taking into account the DSO assets for the proactive management of the distribution system, such as in [3]. More precisely, the proposed work leads to an extension of [3] using an alternative approach to cope with the RES uncertain power production, while supporting the DSO with trade-off solutions and improving the computational performance. The main contributions of the study over the literature are threefold:

- To propose a distinct model for supporting the DSO management of the distribution grid under high levels of variable power production. The modelling of stochastic chance-constrained programming to provide solutions based on trade-off analysis between operating cost and risk (of technical constraints violation), rather than the worst-case conditions modelled by robust optimization in [3];
- To implement a recent AC OPF linearization, improving the computational performance without significantly losing the solution accuracy, in contrast to the nonlinear and nonconvex AC OPF of [3];
- To analyze and compare two distinct linearization techniques when determining the deterministic equivalent problem of the chance-constrained distribution network management problem, highlighting computational and solution efficiency.

1.3. Paper organization

The paper is structured as follows. Section 2 describes the predictive distribution management problem under RES forecast uncertainty. Section 3 details the formulation of the predictive distribution management problem considering a stochastic chance-constrained approach. Section 4 evaluates the proposed model through a 37-bus distribution grid test case based on real data. Section 5 gathers the most important conclusions.

2. Active distribution management

The current grid management procedures of a DSO are becoming insufficient to cope with the uncertainty and variability of RES and extract full value from DER flexibility. Wind and PV penetration into the distribution grid often creates technical problems, such as branch congestion and over/under-voltage problems, and standard DSO tools (like OPF and network reconfiguration standard tools) have difficulties mitigating these events. The research trend is to allow the DSO to seek flexibility among DERs to solve potential congestion and voltage problems. That is, the DSO can pre-identify and use power flexibility from DER (changing the DER operating point) to decongest lines and prevent voltage limit violation.

Within this, the structure of a proactive distribution grid management adapted from [3] is illustrated in Fig. 1. The structure comprises a two-stage problem. The first-stage corresponds to a flexibility market in which the DSO can contract upward and downward flexibility of all available DER at day-ahead horizon. The second-stage is the operating stage in which the DSO manages the grid considering the use of its internal resources (like transformers with on-load tap-changing (OLTC), capacitor banks and storage) and the activation of contracted flexibility under uncertain power generation.

In more detail, the DSO can contract flexibility based on capacity payments in the first-stage. The DER (including RES to some extent) can provide flexibility bids to the DSO since they are actually enabled to control their operating point for upward and downward. Note that RES producers can define their flexibility bids based on their expected availability while accounting for the costs of changing their operating point [26].

In the second-stage, the DSO is responsible for managing the grid, activating all the “reserved” flexibility necessary to solve potential congestion and voltage problems. In this grid management, the DSO is able to control its internal resources, such as transformers with OLTC, capacitor banks and storage systems. We assume that storage systems are owned or managed by the DSO, which provides additional multi-temporal flexibility to the system. To some extent, storage systems are used to reduce the impact of the uncertainty and variability of RES, by absorbing and injecting power to correct the RES deviation in the system.

Moreover, the goal of the proposed model is to enable the DSO to preserve the grid operation and reliability by contracting sufficient flexibility in advance to address potential technical problems that uncertain generation can cause to the grid.

3. Mathematical formulation

In this section, we present the formulation of the predictive distribution management problem considering a two-stage stochastic model based on chance-constrained programming. The aim is to minimize the cost of DER flexibility contracted by the DSO for technical constraints management.

3.1. General problem

The modeling of the distribution management problem must consider the inherent characteristics of the network. Modelling active and reactive power is essential in distribution systems, especially under strong penetration of RES. However, the full AC OPF can be very hard to compute when considering complex problems such as the stochastic optimization with multiple scenarios for RES uncertainty. Thus, a linear-programming approximation of the AC OPF proposed by [27] is implemented.

3.1.1. Objective function

The objective function of the optimization problem can be modeled into two-stages

$$\min_{x,y} \; flex^{DA}(x) + flex^{RT}(y) \tag{1}$$

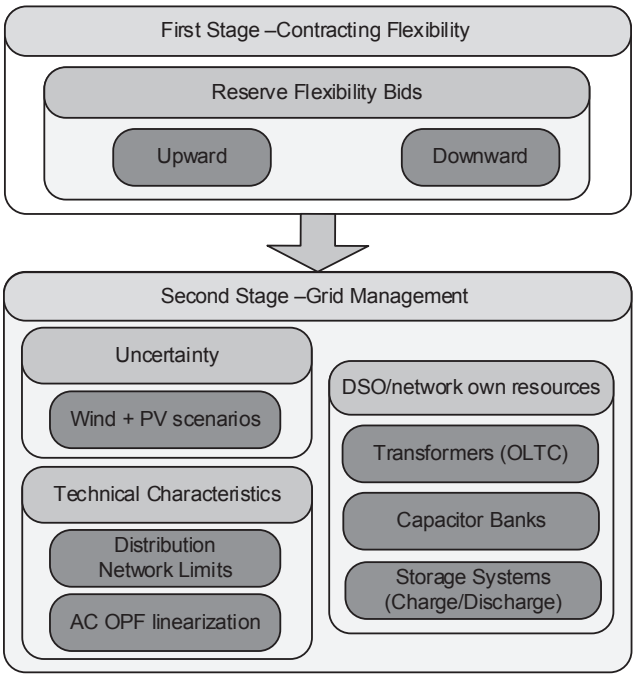

Fig. 1. Proactive distribution management (adapted from [3]).

where $flex^{DA}$ represents the costs for DSO contracting DER flexibility at first-stage to eventually be activated during real-time operation. The flexibility costs at first-stage are defined by the capacity payments for upward and downward flexibility, respectively.

$$flex^{DA}(x) = \sum_{t=1}^{T} \left[\begin{array}{l} \sum_{dg=1}^{N_{DG}} (C^{up}_{DG(dg,t)} P^{up}_{DG(dg,t)} + C^{dw}_{DG(dg,t)} P^{dw}_{DG(dg,t)}) \\ + \sum_{w=1}^{N_W} (C^{up}_{W(w,t)} P^{up}_{W(w,t)} + C^{dw}_{W(w,t)} P^{dw}_{W(w,t)}) + \\ \sum_{pv=1}^{N_{PV}} (C^{up}_{PV(pv,t)} P^{up}_{PV(pv,t)} + C^{dw}_{PV(pv,t)} P^{dw}_{PV(pv,t)}) \\ + \sum_{l=1}^{N_L} (C^{up}_{DR(l,t)} P^{up}_{DR(l,t)} + C^{dw}_{DR(l,t)} P^{dw}_{DR(l,t)}) \end{array} \right] \quad (1.1)$$

Several DERs (namely, DG, wind, PV and demand response (DR)) offers are considered. The decision variable vector × considers the first-stage variables

$$x = \{P^{up}_{DG}, P^{dw}_{DG}, P^{up}_{W}, P^{dw}_{W}, P^{up}_{PV}, P^{dw}_{PV}, P^{up}_{DR}, P^{dw}_{DR}\}.$$

In contrast, the second-stage comprises the activation of the contracted flexibility in any scenario ω, which is given by

$$flex^{RT}(y) = \sum_{t=1}^{T} \sum_{\omega}^{N_\omega} \pi_\omega$$

$$\left[\begin{array}{l} \sum_{dg=1}^{N_{DG}} [C^{act}_{DG(dg,t)} (r^{up}_{DG(dg,t,\omega)} - r^{dw}_{DG(dg,t,\omega)}) + C^{cut}_{DG(dg,t)} P^{cut}_{DG(dg,t,\omega)}] \\ + \sum_{w=1}^{N_W} [C^{act}_{W(w,t)} (r^{up}_{W(w,t,\omega)} - r^{dw}_{W(w,t,\omega)}) + C^{spill}_{W(w,t)} P^{spill}_{W(w,t,\omega)}] + \\ \sum_{pv=1}^{N_{PV}} [C^{act}_{PV(pv,t)} (r^{up}_{PV(pv,t,\omega)} - r^{dw}_{PV(pv,t,\omega)}) + C^{spill}_{PV(pv,t)} P^{spill}_{PV(pv,t,\omega)}] \\ + \sum_{l=1}^{N_L} [C^{act}_{DR(l,t)} (r^{up}_{DR(l,t,\omega)} - r^{dw}_{DR(l,t,\omega)}) + C^{shed}_{L(l,t)} P^{shed}_{L(l,t,\omega)}] + \\ \sum_{st=1}^{N_{ST}} (C_{Dch(st,t)} P_{Dch(st,t,\omega)} - C_{Ch(st,t)} P_{Ch(st,t,\omega)}) \\ + \sum_{cb=1}^{N_{CB}} \sum_{lv=1}^{N_{levels}} C_{CB(cb,t)} |X_{CB(cb,t-1,\omega,lv)} - X_{CB(cb,t,\omega,lv)}| + \\ \sum_{trf=1}^{N_{TRF}} \sum_{lv=1}^{N_{levels}} C_{TRF(trf,t)} |X_{TRF(trf,t-1,\omega,lv)} - X_{TRF(trf,t,\omega,lv)}| \end{array} \right] \quad (1.2)$$

where additional operating costs for balancing the system are considered, using DSO owned resources. This might include storage units (if regulatory framework allows), capacitor banks and transformers with OLTC ability. More precisely, the activation of flexibility corresponds to the amount of up/down power scheduled for scenario ω, which changes the operating point of the resource. In what concerns to the scenario generation and probabilities, quantile forecast of wind and PV were used to generate scenarios considering spatial-temporal correlation as in [28]. It is worth mentioning that scenario generation is modeled independently for wind and PV, which means that wind and PV uncertain variables are not related. Thus, a complete combination of the two sets is determined by considering a uniform probability for each scenario. Therefore, the scenario reduction of the full set of scenarios is performed following [29] approach. The second-stage variables are summarized in the vector y

$$y = \left\{ \begin{array}{l} r^{up}_{DG}, r^{dw}_{DG}, P^{cut}_{DG}, r^{up}_{W}, r^{dw}_{W}, P^{spill}_{W}, r^{up}_{PV}, r^{dw}_{PV}, P^{spill}_{PV}, r^{up}_{DR}, r^{dw}_{DR}, P^{shed}_{L}, P_{Dch} \\ , P_{Ch}, X_{CB}, X_{TRF}, X_{ST}, \\ Q_{DG}, Q_L, Q_{SU}, SOC, \Delta V_{TRF}, V_{sb}, V_{ij}, P_{Flow}, PWL_{ij}, \theta_{ij}, Q_{Flow}, X^{CC} \\ , P^{Total}_{DG}, \widetilde{P}^{Total}_{DG}, P^{Total}_{SU}, \widetilde{P}^{Total}_{SU}, \\ P^{Total}_{W}, \widetilde{P}^{Total}_{W}, P^{Total}_{ST}, \widetilde{P}^{Total}_{ST}, P^{Total}_{W}, \widetilde{P}^{Total}_{W}, P^{Total}_{PV}, \widetilde{P}^{Total}_{PV}, P^{Total}_{L}, \widetilde{P}^{Total}_{L} \\ , P^{Total}_{Flow}, \widetilde{P}^{Total}_{Flow} Z_{CB}, Z_{TRF} \end{array} \right\}$$

The objective function is subjected to several first-stage and second-stage constraints.

3.1.2. First-stage constraints

The first-stage constraints consider the upper bound of upward (2.1) and downward (2.2) flexibility offers transmitted by DG units.

$$P^{up}_{DG(dg,t)} \leqslant P^{bid\_up}_{DG(dg,t)} \quad \forall\, t \in \{1, ...,T\}, \forall\, dg \in \{1, ...,N_{DG}\}, \quad (2.1)$$

$$P^{dw}_{DG(dg,t)} \leqslant P^{bid\_dw}_{DG(dg,t)} \quad \forall\, t \in \{1, ...,T\}, \forall\, dg \in \{1, ...,N_{DG}\}, \quad (2.2)$$

Wind and PV aggregators also provide upward and downward flexibility offers. Thus, it is assumed that wind power producers have the ability to provide upward flexibility as in [30]. The wind power producer is also able to reduce active power production when activated by the DSO. However, the operating point $P^{op}_{W(w,t)}$ of the wind power producer established in the electrical energy market limits the downward wind power offer (2.3). The upper bound of the upward wind power offer is given in (2.4).

$$P^{dw}_{W(w,t)} \leqslant P^{op}_{W(w,t)} \quad \forall\, t \in \{1, ...,T\}, \forall\, w \in \{1, ...,N_W\}, \quad (2.3)$$

$$P^{up}_{W(w,t)} \leqslant P^{bid\_up}_{W(w,t)} \quad \forall\, t \in \{1, ...,T\}, \forall\, w \in \{1, ...,N_W\}, \quad (2.4)$$

Note that both (2.3) and (2.4) constraints are also applied to PV aggregators. In parallel, upper bounds for DR aggregators provide offers for upward (2.5) and downward (2.6) flexibility are expressed as

$$P^{up}_{DR(l,t)} \leqslant P^{bid\_up}_{DR(l,t)} \quad \forall\, t \in \{1, ...,T\}, \forall\, l \in \{1, ...,N_L\}, \quad (2.5)$$

$$P^{dw}_{DR(l,t)} \leqslant P^{bid\_dw}_{DR(l,t)} \quad \forall\, t \in \{1, ...,T\}, \forall\, l \in \{1, ...,N_L\}, \quad (2.6)$$

where $P^{bid\_up}_{DR(l,t)}$ and $P^{bid\_dw}_{DR(l,t)}$ are the maximum amount of load that can be reduced or increased, respectively. It is considered that the load can be reduced P^{up}_{DR} or increased P^{dw}_{DR}, according to the system needs. Moreover, the load reduction/increase is assumed to be based on the type of direct load control of the demand response.

3.1.3. Second-stage constraints

The second-stage consider all the stochastic constraints dependent of scenario ω. This includes equality and inequality constraints representative of: the upper bounds of upward and downward flexibility of all resources (3.1)–(3.9); active and reactive power consumption (3.10) and (3.11); energy storage systems limits and balance (3.12)–(3.15); capacitor banks limits and tap-changing (3.16) and (3.17); transformers limits with OLTC (3.18)–(3.23); active and reactive power balance (3.24)–(3.28); limits of voltage magnitude (3.29); and lines thermal capacity (3.30)–(3.32).

The activation of upward and downward flexibility for DG units is limited by the upward and downward offer contracted in the first-stage,

respectively. In parallel, the generation curtailment power is constrained by the difference between the current operating point and the downward offer of the DG unit, hence

$$r^{up}_{DG(dg,t,\omega)} \leqslant P^{up}_{DG(dg,t)}, \quad \forall\, t \in \{1, ...,T\}, \forall\, dg \in \{1, ...,N_{DG}\}, \forall\, \omega \in \{1, ...,N_{\omega}\} \tag{3.1}$$

$$r^{dw}_{DG(dg,t,\omega)} \leqslant P^{dw}_{DG(dg,t)}, \quad \forall\, t \in \{1, ...,T\}, \forall\, dg \in \{1, ...,N_{DG}\}, \forall\, \omega \in \{1, ...,N_{\omega}\} \tag{3.2}$$

$$P^{cut}_{DG(dg,t,\omega)} \leqslant P^{op}_{DG(dg,t)} - r^{dw}_{DG(dg,t,\omega)}, \quad \forall\, t \in \{1, ...,T\}, \forall\, dg \in \{1, ...,N_{DG}\}, \forall\, \omega \in \{1, ...,N_{\omega}\} \tag{3.3}$$

The reactive power production of DG units is dependent of the active power production. This is modelled considering the operating point established in the first-stage plus the upward and downward flexibility and power curtailment in the second-stage with a fixed tan $\phi = 0.3$ [31].

$$Q_{DG(dg,t,\omega)} = (P^{op,i}_{DG(dg,t)} + r^{up,i}_{DG(dg,t,\omega)} - r^{dw,i}_{DG(dg,t,\omega)} - P^{cut}_{DG(dg,t,\omega)}) \tan\phi, \quad \forall\, t \in \{1, ...,T\}, \forall\, dg \in \{1, ...,N_{DG}\}, \forall\, \omega \in \{1, ...,N_{\omega}\} \tag{3.4}$$

Similarly, the activation of upward and downward flexibility of wind and PV aggregators is constrained by the contracted power in the first-stage. Additionally, the wind spillage is modelled by the difference between the wind operating point plus the wind power deviation, and the wind downward activation (3.7). The modeling of PV aggregators also includes these constraints.

$$r^{up}_{W(w,t,\omega)} \leqslant P^{up}_{W(w,t)}, \quad \forall\, t \in \{1, ...,T\}, \forall\, w \in \{1, ...,N_{W}\}, \forall\, \omega \in \{1, ...,N_{\omega}\} \tag{3.5}$$

$$r^{dw}_{W(w,t,\omega)} \leqslant P^{dw}_{W(w,t)}, \quad \forall\, t \in \{1, ...,T\}, \forall\, w \in \{1, ...,N_{W}\}, \forall\, \omega \in \{1, ...,N_{\omega}\} \tag{3.6}$$

$$P^{spill}_{W(w,t,\omega)} \leqslant P^{op}_{W(w,t)} - r^{dw}_{W(w,t,\omega)} + \Delta P_{W(w,t,\omega)}, \quad \forall\, t \in \{1, ...,T\}, \forall\, w \in \{1, ...,N_{W}\}, \forall\, \omega \in \{1, ...,N_{\omega}\} \tag{3.7}$$

In contrast, the activation of upward and downward DR offers is constrained by

$$r^{up}_{DR(l,t,\omega)} \leqslant P^{up}_{DR(l,t)}, \quad \forall\, t \in \{1, ...,T\}, \forall\, l \in \{1, ...,N_{L}\}, \forall\, \omega \in \{1, ...,N_{\omega}\} \tag{3.8}$$

$$r^{dw}_{DR(l,t,\omega)} \leqslant P^{dw}_{DR(l,t)}, \quad \forall\, t \in \{1, ...,T\}, \forall\, l \in \{1, ...,N_{L}\}, \forall\, \omega \in \{1, ...,N_{\omega}\} \tag{3.9}$$

$$P^{shed}_{L(l,t,\omega)} \leqslant P_{L(l,t)} - P^{op}_{DR(l,t)} - r^{up}_{DR(l,t,\omega)}, \quad \forall\, t \in \{1, ...,T\}, \forall\, l \in \{1, ...,N_{L}\}, \forall\, \omega \in \{1, ...,N_{\omega}\} \tag{3.10}$$

where (3.10) represents the load shedding constrained by the active power consumption of the respective load. The reactive power consumption is determined based on the active power consumption plus the upward and downward flexibility of DR and load shedding of load l considering tan $\phi = 0.3$ [32].

$$Q_{L(l,t,\omega)} = (P_{L(l,t)} - P^{op}_{DR(l,t)} + r^{dw}_{DR(l,t,\omega)} - r^{up}_{DR(l,t,\omega)} - P^{shed}_{L(l,t,\omega)}) \tan\phi, \quad \forall\, t \in \{1, ...,T\}, \forall\, l \in \{1, ...,N_{L}\}, \forall\, \omega \in \{1, ...,N_{\omega}\} \tag{3.11}$$

Other network resources such as storage units, capacitor banks and transformers concerns different characteristics and therefore modelling. The ESS combines different constraints such as the upper and lower limits for charging (3.12) and discharging (3.13), upper and lower bounds of energy stored in the battery (3.14), and energy balance of the battery (3.15).

$$P_{Ch(st,t,\omega)} \leqslant P^{Max}_{Ch(st,t)} X_{ST(st,t,\omega)}, \quad \forall\, t \in \{1, ...,T\}, \forall\, st \in \{1, ...,N_{ST}\}, \forall\, \omega \in \{1, ...,N_{\omega}\} \tag{3.12}$$

$$P_{Dch(st,t,\omega)} \leqslant P^{Max}_{Dch(st,t)} (1 - X_{ST(st,t,\omega)}), \quad \forall\, t \in \{1, ...,T\}, \forall\, st \in \{1, ...,N_{ST}\}, \forall\, \omega \in \{1, ...,N_{\omega}\} \tag{3.13}$$

$$E_{Min(st,t)} \leqslant SOC_{(st,t,\omega)} \leqslant E_{BatCap(st,t,\omega)}, \quad \forall\, t \in \{1, ...,T\}, \forall\, st \in \{1, ...,N_{ST}\}, \forall\, \omega \in \{1, ...,N_{\omega}\} \tag{3.14}$$

$$SOC_{(st,t,\omega)} = SOC_{(st,t-1,\omega)} + \eta_{Ch(st)} P_{Ch(st,t,\omega)} - \frac{1}{\eta_{Dch(st)}} P_{Dch(st,t,\omega)}, \quad \forall\, t \in \{1, ...,T\}, \forall\, st \in \{1, ...,N_{ST}\}, \forall\, \omega \in \{1, ...,N_{\omega}\} \tag{3.15}$$

The energy balance of the storage takes into account the state of charge in the previous period, thereby considering the multi-temporal characteristics of modeling ESS. Another important component in distribution grids is the capacitor banks, located at the substation that allows adjusting the injection of reactive power in the network. The modelling of this resource assumes the tap-changing characteristics and that the DSO owns the equipment. Thus, capacitor banks can be modelled as

$$Q_{CB(cb,t,\omega,lv)} = Q^{levels}_{CB(cb,t,lv)} X_{CB(cb,t,\omega,lv)}, \quad \forall\, t \in \{1, ...,T\}, \quad \forall\, cb \in \{1, ...,N_{CB}\}, \forall\, \omega \in \{1, ...,N_{\omega}\}, \forall\, lv \in \{1, ...,N_{levels}\} \tag{3.16}$$

$$\sum_{lv=1}^{N_{levels}} X_{CB(cb,t,\omega,lv)} = 1, \quad \forall\, t \in \{1, ...,T\}, \forall\, cb \in \{1, ...,N_{CB}\}, \forall\, \omega \in \{1, ...,N_{\omega}\} \tag{3.17}$$

Similarly, the DSO also owns transformers with OLTC ability. It is assumed that the voltage impact of each tap-changing level in the secondary bus of the transformer is known, and is constrained by

$$\Delta V_{TRF(trf,t,\omega,lv)} = V^{levels}_{TRF(trf,t,lv)} X_{TRF(trf,t,\omega,lv)}, \quad \forall\, t \in \{1, ...,T\}, \forall\, \omega \in \{1, ...,N_{\omega}\}, \forall\, trf \in \{1, ...,N_{TRF}\}, \forall\, lv \in \{1, ...,N_{levels}\} \tag{3.18}$$

$$\sum_{lv=1}^{N_{levels}} X_{TRF(trf,t,\omega,lv)} = 1, \quad \forall\, t \in \{1, ...,T\}, \forall\, \omega \in \{1, ...,N_{\omega}\}, \forall\, trf \in \{1, ...,N_{TRF}\} \tag{3.19}$$

$$V_{sb(t,\omega)} = V^{ref}_{sb(t,\omega)} + \sum_{lv=1}^{N_{levels}} X_{TRF(trf,t,\omega,lv)}, \quad \forall\, t \in \{1, ...,T\}, \forall\, \omega \in \{1, ...,N_{\omega}\}, \forall\, trf \in \{1, ...,N_{TRF}\} \tag{3.20}$$

where $\Delta V_{TRF(trf,t,\omega,lv)}$ is the voltage level of the tap-changing in the transformer, while $V^{levels}_{TRF(trf,t,lv)}$ sets all available levels of the OLTC ability of that transformer. The selection and activation of the levels is made through the binary variable $X_{TRF(trf,t,\omega,lv)}$. The transformer also limits the active and reactive power that comes from upstream connection to the grid. This condition is modelled through a quadratic constraint. However, it is used a piecewise linear approximation of the quadratic function, as in [27], to reduce the complexity of the problem. Hence,

$$0 \geqslant 2Px^{i}_{(t,k)} \left(\sum_{su=1}^{N_{SU}} P^{i}_{SU(su,t,\omega)} - Px^{i}_{(t,k)} \right) + 2Py^{i}_{(t,k)} \left(\sum_{su=1}^{N_{SU}} Q^{i}_{SU(su,t,\omega)} - Py^{i}_{(t,k)} \right), \quad \forall\, t \in \{1, ...,T\}, \forall\, i \in \{1, ...,N_{Bus}\}, \forall\, \omega \in \{1, ...,N_{\omega}\}, \forall\, k \in \{1, ...,N_{k}\} \tag{3.21}$$

$$Px^{i}_{(t,k)} = \sum_{trf=1}^{N_{TRF}} S^{Max}_{trf} \cos(ang_{k}), \quad \forall\, t \in \{1, ...,T\}, \forall\, i \in \{1, ...,N_{Bus}\}, \forall\, k \in \{1, ...,N_{k}\} \tag{3.22}$$

$$Py^{i}_{(t,k)} = \sum_{trf=1}^{N_{TRF}} S^{Max}_{trf} sin(ang_k), \qquad \forall\, t \in \{1, ...,T\}, \forall\, i \in \{1, ...,N_{Bus}\}, \forall\, k \in \{1, ...,N_k\} \tag{3.23}$$

where ang_k is a k number of angles between 0 and 2π representative of the piecewise linear slopes. Following [27], four to seven piecewise linear slopes are sufficient to fairly approximate the apparent power quadratic function.

In this problem a linear programming approximation of the traditional AC OPF has been applied based on [27] and formulated on equations (3.24)–(3.32). For more details on the assumptions of the AC OPF linearization, interested readers are directed to [27]. Future work may comprise the comparison of distinct convex relaxations of the AC OPF, such as [33]. One of the main challenges of a DSO in conducting active distribution management under uncertainty is to ensure inexpensive solutions that keep the system operation under proper confidence levels of operation. Chance-constrained programming allows to model feasible regions of the problem under the probability level (risk) defined by the DSO. Thus, chance-constrained optimization can constrain the impact of unusual operating scenarios with a low probability of occurring in the solution. In other words, unusual operating scenarios can increase the contract of high flexibility levels, resulting in high costs to the DSO to achieve low risk levels. In this scope, chance-constrained optimization has been applied to the active power balance constraint, since it ensures that the probability of load imbalance is less than a predefined risk level ε. Therefore, the decision-maker can control the risk level ε that gives the desired trade-off between cost and reliability.

Nevertheless, the chance-constrained programming can be applied to other constraints of the active distribution management problem, such as reactive power balance. On the one hand, the inclusion of this chance-constraint will bring more flexibility to the proposed solution, however, it is not critical to this problem, since the DSO has static equipment (e.g. capacitor banks) to solve reactive power issues, as well as DER will bring more flexibility to the reactive power management problem. On the other hand, the chance-constraint will bring more complexity to the problem and, therefore, will increase the computational effort to obtain a good solution. Future work will focus on this subject. Thus, the probability constraint of the active power balance is given by

$$\Pr\left[\begin{array}{l} \sum_{dg=1}^{N_{DG}} (P^{op,i}_{DG(dg,t)} + r^{up,i}_{DG(dg,t,\omega)} - r^{dw,i}_{DG(dg,t,s)} - P^{cut}_{DG(dg,t,\omega)}) + \sum_{su=1}^{N_{SU}} P^{i}_{SU(su,t,\omega)} \\ \quad + \sum_{st=1}^{N_{ST}} (P^{i}_{Dch(st,t,\omega)} - P^{i}_{Ch(st,t,\omega)}) + \\ \sum_{w=1}^{N_W} (P^{op,i}_{W(w,t)} + \Delta P^{i}_{W(w,t,\omega)} + r^{up,i}_{W(w,t,\omega)} - r^{dw,i}_{W(w,t,\omega)} - P^{spill,i}_{W(w,t,\omega)}) \\ \quad + \sum_{pv=1}^{N_{PV}} (P^{op,i}_{PV(pv,t)} + \Delta P^{i}_{PV(pv,t,\omega)} + r^{up,i}_{PV(pv,t,\omega)} - r^{dw,i}_{PV(pv,t,\omega)} - P^{spill,i}_{PV(pv,t,\omega)}) \\ \sum_{l=1}^{N_L} (P^{op,i}_{DR(l,t)} + r^{up,i}_{DR(l,t,\omega)} - r^{dw,i}_{DR(l,t,\omega)} + P^{shed,i}_{L(l,t,\omega)} - P^{i}_{L(l,t)}) - \sum_{j \in N_{bus}}^{i \neq j} P^{i,j}_{Flow(t,\omega)} \\ \quad = 0, \\ \qquad t \in \{1, ...,T\}, \forall\, i,j \in \{1, ...,N_{Bus}\}, \forall\, \omega \in \{1, ...,N_\omega\} \end{array}\right] \geqslant 1 - \varepsilon \tag{3.24}$$

where P_{Flow} represents the active power that flows through the lines of the network, which is given by

$$P^{i,j}_{Flow(t,\omega)} = G_{ij} - G_{ij} PWL_{ij(t,\omega)} - B_{ij}(\theta_{ij(t,\omega)}), \qquad \forall\, t \in \{1, ...,T\}, \forall\, i,j \in \{1, ...,N_{Bus}\}, \forall\, \omega \in \{1, ...,N_\omega\}, \theta_{ij(t,\omega)} = \theta_{i(t,\omega)} - \theta_{j(t,\omega)} \tag{3.25}$$

and *PWL* is the piecewise linear approximation of the cosine function as shown in [27]. $\theta_{i,j}$ is the phase angle difference between bus *i* and *j*. The PWL is represented as

$$PWL_{ij(t,\omega)} \leqslant -\sin(ang_k)(\theta_{ij(t,\omega)} - ang_k) + \cos(ang_k), \quad \forall\, t \in \{1, ...,T\}, \forall\, i,j \in \{1, ...,N_{Bus}\}, \forall\, \omega \in \{1, ...,N_\omega\}, \forall\, k \in \{1, ...,N_k\}, \theta_{ij(t,\omega)} = \theta_{i(t,\omega)} - \theta_{j(t,\omega)} \tag{3.26}$$

where ang_a depicts the number of angles between $-\pi/3$ and $\pi/3$ representative of the piecewise linear slopes for the cosine function. In parallel, the reactive power balance refers to the reactive power generation and consumption in the system and is modelled as

$$\sum_{dg=1}^{N_{DG}} (Q^{i}_{DG(dg,t,\omega)}) - \sum_{l=1}^{N_L} Q^{i}_{L(l,t)} + \sum_{su=1}^{N_{SU}} Q^{i}_{SU(su,t,\omega)} + \sum_{cb=1}^{N_{CB}} \sum_{lv=1}^{N_{levels}} Q^{i}_{CB(cb,t,\omega,lv)} - \sum_{j \in N_{bus}}^{i \neq j} Q^{i,j}_{Flow(t,\omega)} = 0 \quad , \forall\, t \in \{1, ...,T\}, \forall\, i,j \in \{1, ...,N_{Bus}\}, \forall\, \omega \in \{1, ...,N_\omega\}, \theta_{ij(t,\omega)} = \theta_{i(t,\omega)} - \theta_{j(t,\omega)} \tag{3.27}$$

where Q_{Flow} represents the reactive power that flows through he lines of the network, which is modelled as

$$Q^{i,j}_{Flow(t,\omega)} = -B_{ij} - G_{ij}\theta_{ij(t,\omega)} + B_{ij} PWL_{ij(t,\omega)} - B_{ij} V_{ij(t,\omega)}, \quad t \in \{1, ...,T\}, \forall\, i,j \in \{1, ...,N_{Bus}\}, \forall\, \omega \in \{1, ...,N_\omega\}, \theta_{ij(t,\omega)} = \theta_{i(t,\omega)} - \theta_{j(t,\omega)}, V_{ij(t,\omega)} = V_{i(t,\omega)} - V_{j(t,\omega)} \tag{3.28}$$

and V_{ij} is the voltage change on bus *i,j*. The voltage in each bus is limited by the upward and downward bound as

$$V^{i}_{Min} \leqslant V_{i(t,\omega)} \leqslant V^{i}_{Max}, \qquad \forall\, t \in \{1, ...,T\}, \forall\, \omega \in \{1, ...,N_\omega\}, \forall\, i,j \in \{1, ...,N_B\} \tag{3.29}$$

Similar to the apparent power constraint of transformers (3.21)–(3.23), the thermal line limit takes into account both active and reactive power flow. Thus, the piecewise linear approximation of the quadratic function entails

$$0 \geqslant 2Px^{i}_{(t,k)}(P^{i,j}_{Flow(t,\omega)} - Px^{i}_{(t,k)}) + 2Py^{i}_{(t,k)}(Q^{i,j}_{Flow(t,\omega)} - Py^{i}_{(t,k)}) \ , \quad \forall\, t \in \{1, ...,T\}, \forall\, i,j \in \{1, ...,N_{Bus}\}, \forall\, \omega \in \{1, ...,N_\omega\}, \forall\, k \in \{1, ...,N_k\} \tag{3.30}$$

$$Px^{i}_{(t,k)} = S^{Max}_{ij} \cos(ang_k), \qquad \forall\, t \in \{1, ...,T\}, \forall\, i,j \in \{1, ...,N_{Bus}\}, \forall\, k \in \{1, ...,N_k\} \tag{3.31}$$

$$Py^{i}_{(t,k)} = S^{Max}_{ij} sin(ang_k), \qquad \forall\, t \in \{1, ...,T\}, \forall\, i,j \in \{1, ...,N_{Bus}\}, \forall\, k \in \{1, ...,N_k\} \tag{3.32}$$

3.2. Chance-constrained reformulation

The chance-constrained programming can be formulated and solved using many different ways [34–37]. One of the ways is to reformulate and solve the chance-constrained problem through the formulation of the deterministic equivalent problem via integer programming methods. Within this variation of chance-constrained programming, the deterministic equivalent of the chance constraint can be obtained by using the Big-M method, introducing a binary variable [34] or through bilinear reformulation [35]. Thus, the reformulation of the chance constraint (3.24) through the Big-M method can be rewritten as follows

$$
\begin{aligned}
&- M X^{CC}_{(t,\omega)} \leqslant \sum_{dg=1}^{N_{DG}} (P^{op,i}_{DG(dg,t)} + r^{up,i}_{DG(dg,t,\omega)} - r^{dw,i}_{DG(dg,t,s)} - P^{cut}_{DG(dg,t,\omega)}) \\
&\quad + \sum_{su=1}^{N_{SU}} P^{i}_{SU(su,t,\omega)} + \sum_{st=1}^{N_{ST}} (P^{i}_{Dch(st,t,\omega)} - P^{i}_{Ch(st,t,\omega)}) + \\
&\sum_{w=1}^{N_W} (P^{op,i}_{W(w,t)} + \Delta P^{i}_{W(w,t,\omega)} + r^{up,i}_{W(w,t,\omega)} - r^{dw,i}_{W(w,t,\omega)} - P^{spill,i}_{W(w,t,\omega)}) \\
&\quad + \sum_{pv=1}^{N_{PV}} (P^{op,i}_{PV(pv,t)} + \Delta P^{i}_{PV(pv,t,\omega)} + r^{up,i}_{PV(pv,t,\omega)} - r^{dw,i}_{PV(pv,t,\omega)} \\
&\quad - P^{spill,i}_{PV(pv,t,\omega)}) + \\
&\sum_{l=1}^{N_L} (P^{op,i}_{DR(l,t)} + r^{up,i}_{DR(l,t,\omega)} - r^{dw,i}_{DR(l,t,\omega)} + P^{shed,i}_{L(l,t,\omega)} - P^{i}_{L(l,t)}) - \sum_{j \in N_{bus}}^{i \neq j} P^{i,j}_{Flow(t,\omega)} \leqslant \\
&M X^{CC}_{(t,\omega)}, \\
&\qquad t \in \{1, ...,T\}, \forall\, i, j \in \{1, ...,N_{Bus}\}, \forall\, \omega \in \{1, ...,N_{\omega}\}
\end{aligned}
\tag{4.1}
$$

$$
\sum_{\omega}^{N_{\omega}} \pi_{\omega} X^{CC}_{(t,\omega)} \leqslant \varepsilon, \qquad \forall\, t \in \{1, ...,T\} \tag{4.2}
$$

where M is a sufficiently large number and X^{CC} is the binary variable that indicates if for a certain period t and scenario ω, the active power balance equation is met ($X^{CC} = 0$) or if it is relaxed to the boundaries M ($X^{CC} = 1$). It is well known that the Big-M method reformulation has significant issues, like the challenging of estimating the value of M. The value of M should be sufficiently high to allow for a good convergence solution. In addition, the Big-M formulation slows down the computational performance, which may not be the best solution for the reformulation of the chance-constrained problem.

Another way to convert the chance-constrained problem to the deterministic one is to use bilinear reformulation. Following [34,35], the bilinear mixed integer reformulation is given by

$$
\begin{aligned}
&\left(\begin{array}{l}
\sum_{dg=1}^{N_{DG}} (P^{op,i}_{DG(dg,t)} + r^{up,i}_{DG(dg,t,\omega)} - r^{dw,i}_{DG(dg,t,s)} - P^{cut}_{DG(dg,t,\omega)}) \\
\quad + \sum_{su=1}^{N_{SU}} P^{i}_{SU(su,t,\omega)} + \sum_{st=1}^{N_{ST}} (P^{i}_{Dch(st,t,\omega)} - P^{i}_{Ch(st,t,\omega)}) + \\
\sum_{w=1}^{N_W} (P^{op,i}_{W(w,t)} + \Delta P^{i}_{W(w,t,\omega)} + r^{up,i}_{W(w,t,\omega)} - r^{dw,i}_{W(w,t,\omega)} \\
\quad - P^{spill,i}_{W(w,t,\omega)}) + \sum_{pv=1}^{N_{PV}} (P^{op,i}_{PV(pv,t)} + \Delta P^{i}_{PV(pv,t,\omega)} + r^{up,i}_{PV(pv,t,\omega)} \\
\quad - r^{dw,i}_{PV(pv,t,\omega)} - P^{spill,i}_{PV(pv,t,\omega)}) + \\
\quad \sum_{l=1}^{N_L} (P^{op,i}_{DR(l,t)} + r^{up,i}_{DR(l,t,\omega)} - r^{dw,i}_{DR(l,t,\omega)} + P^{shed,i}_{L(l,t,\omega)} - P^{i}_{L(l,t)}) \\
\quad - \sum_{j \in N_{bus}}^{i \neq j} P^{i,j}_{Flow(t,\omega)}
\end{array} \right) (1 - X^{CC}_{(t,\omega)}) \\
&= 0, \\
&\qquad t \in \{1, ...,T\}, \forall\, i, j \in \{1, ...,N_{Bus}\}, \forall\, \omega \in \{1, ...,N_{\omega}\}
\end{aligned}
\tag{4.3}
$$

$$
\sum_{\omega}^{N_{\omega}} \pi_{\omega} X^{CC}_{(t,\omega)} \leqslant \varepsilon, \qquad \forall\, t \in \{1, ...,T\} \tag{4.4}
$$

where the balance equation is met when $X^{CC} = 0$, and ignored when $X^{CC} = 1$. The bilinear reformulation makes the problem non-linear. However, the constraint can be converted to linear by applying the McCormick relaxation method [38]. For simplicity, let's assume that all distributed generation variables are reduced to

$$
P^{Total,i}_{DG(dg,t,\omega)} = P^{op,i}_{DG(dg,t)} + r^{up,i}_{DG(dg,t,\omega)} - r^{dw,i}_{DG(dg,t,s)} - P^{cut}_{DG(dg,t,\omega)}, \quad \forall\, dg \in \{1, ...,N_{DG}\}, \forall\, t \in \{1, ...,T\}, \forall\, \omega \in \{1, ...,N_{\omega}\} \tag{4.5}
$$

Similar assumption is applied to the variables of external suppliers, storage, wind, PV, loads and power flow in the lines, hence (4.3) is reduced to

$$
\begin{aligned}
&\left(\begin{array}{l}
\sum_{dg=1}^{N_{DG}} P^{Total,i}_{DG(dg,t,\omega)} + \sum_{su=1}^{N_{SU}} P^{Total,i}_{SU(su,t,\omega)} + \sum_{st=1}^{N_{ST}} P^{Total,i}_{ST(st,t,\omega)} + \\
\quad \sum_{w=1}^{N_W} P^{Total,i}_{W(w,t,\omega)} + \sum_{pv=1}^{N_{PV}} P^{Total,i}_{PV(pv,t,\omega)} + \sum_{l=1}^{N_L} P^{Total,i}_{L(l,t,\omega)} \\
\quad - \sum_{j \in N_{bus}}^{i \neq j} P^{i,j,Total}_{Flow(t,\omega)}
\end{array} \right) (1 - X^{CC}_{(t,\omega)}) \\
&= 0, \\
&\qquad t \in \{1, ...,T\}, \forall\, i, j \in \{1, ...,N_{Bus}\}, \forall\, \omega \in \{1, ...,N_{\omega}\}
\end{aligned}
\tag{4.6}
$$

then, McCormick relaxation can be applied assuming that the bilinear term $P^{Total}X^{CC} = P^{Total}$ is linearized through including the constraints (4.8)–(4.10)

$$
\begin{aligned}
&\sum_{dg=1}^{N_{DG}} (P^{Total,i}_{DG(dg,t,\omega)} - \widetilde{P}^{Total,i}_{DG(dg,t,\omega)}) + \sum_{su=1}^{N_{SU}} (P^{Total,i}_{SU(su,t,\omega)} - \widetilde{P}^{Total,i}_{SU(su,t,\omega)}) \\
&+ \sum_{st=1}^{N_{ST}} (P^{Total,i}_{ST(st,t,\omega)} - \widetilde{P}^{Total,i}_{ST(st,t,\omega)}) + \sum_{w=1}^{N_W} (P^{Total,i}_{W(w,t,\omega)} - \widetilde{P}^{Total,i}_{W(w,t,\omega)}) + \\
&\sum_{pv=1}^{N_{PV}} (P^{Total,i}_{PV(pv,t,\omega)} - \widetilde{P}^{Total,i}_{PV(pv,t,\omega)}) + \sum_{l=1}^{N_L} (P^{Total,i}_{L(l,t,\omega)} - \widetilde{P}^{Total,i}_{L(l,t,\omega)}) \\
&\quad - \sum_{j \in N_{bus}}^{i \neq j} (P^{i,j,Total}_{Flow(t,\omega)} - \widetilde{P}^{i,j,Total}_{Flow(t,\omega)}) = 0, \\
&\quad t \in \{1, ...,T\}, \forall\, i, j \in \{1, ...,N_{Bus}\}, \forall\, \omega \in \{1, ...,N_{\omega}\}
\end{aligned}
\tag{4.7}
$$

$$
P^{Min}_{DG(dg,t)} X^{CC}_{(t,\omega)} \leqslant \widetilde{P}^{Total,i}_{DG(dg,t,\omega)} \leqslant P^{Max}_{DG(dg,t)} X^{CC}_{(t,\omega)}, \qquad \forall\, dg \in \{1, ...,N_{DG}\}, t \in \{1, ...,T\}, \forall\, \omega \in \{1, ...,N_{\omega}\} \tag{4.8}
$$

$$
\widetilde{P}^{Total,i}_{DG(dg,t,\omega)} \leqslant P^{Total,i}_{DG(dg,t,\omega)} + P^{Min}_{DG(dg,t)} (X^{CC}_{(t,\omega)} - 1), \qquad \forall\, dg \in \{1, ...,N_{DG}\}, t \in \{1, ...,T\}, \forall\, \omega \in \{1, ...,N_{\omega}\} \tag{4.9}
$$

$$
\widetilde{P}^{Total,i}_{DG(dg,t,\omega)} \geqslant P^{Total,i}_{DG(dg,t,\omega)} + P^{Max}_{DG(dg,t)} (X^{CC}_{(t,\omega)} - 1), \qquad \forall\, dg \in \{1, ...,N_{DG}\}, t \in \{1, ...,T\}, \forall\, \omega \in \{1, ...,N_{\omega}\} \tag{4.10}
$$

where P^{Min} and P^{Max} are the minimum and maximum limits of generation of the distributed generation dg, respectively. Note that Eqs. (4.8)–(4.10) must also be applied to the remaining bilinear terms.

3.3. Absolute function reformulation

The absolute function modelled in the objective function can be reformulated via linear programming by adding a new variable and two additional constraints, like in [39]. Thus, the absolute function considering the tap position of the capacitor banks can be rewritten as

$$
\min \sum_{cb=1}^{N_{CB}} \sum_{lv=1}^{N_{levels}} C_{CB(cb,t)} Z_{CB(cb,t,\omega,lv)} \qquad s.\,t. \tag{5.1}
$$

$$
X_{CB(cb,t-1,\omega,lv)} - X_{CB(cb,t,\omega,lv)} \leqslant Z_{CB(cb,t,\omega,lv)} \tag{5.2}
$$

$$
X_{CB(cb,t,\omega,lv)} - X_{CB(cb,t-1,\omega,lv)} \leqslant Z_{CB(cb,t,\omega,lv)}, \quad \forall\, t \in \{1, ...,T\}, \forall\, cb \in \{1, ...,N_{CB}\}, \forall\, \omega \in \{1, ...,N_{\omega}\}, \forall\, lv \in \{1, ...,N_{levels}\} \tag{5.3}
$$

where Z is a positive variable limited by the positive and negative value of the absolute function. This linear approximation is also used to linearize the absolute function related to the tap changing of transformers in the objective function.

4. Test case

A case study illustrating the applicability and performance of the proposed model, accounting for a variety of uncertain situations is

presented in this section.

4.1. Outline

The case study is based on the work presented in [3], which considers a distribution network with an energy mix of 2050, as shown in Fig. 2.

This 11 kV distribution network has 37 bus with a single upstream connection to the high voltage network through two power transforms of 10 MVA each. In this analysis, we assume that the DERs are aggregated by technology, thus each aggregator represents a specific type of DER technology. However, the model has been designed to cope with aggregators considering mixed portfolio. In addition, 22 consumption points with aggregated demand and DR programs are considered. Consumption profiles and network location were taken from [3]. Furthermore, it is assumed that the DSO operates transformers with OLTC, capacitor banks and energy storage systems to support grid management. Characteristics of transformers and capacitor banks, as well as costs were taken from [3]. Capacitor banks can reach a maximum reactive power of 0.8 MVAr. Similarly, ESS units share the same features as in [3]. Both charge $\hat{\Gamma}_{\cdot Ch}$ and discharge $\hat{\Gamma}_{\cdot Dch}$ efficiency coefficients are equal to 0.8. The general characteristics and operating point of all DER aggregators are presented in Table 1.

The DER operating point represents their scheduled bids in the energy market, which is used as the current state of the units in the system before optimization of the grid management. All DERs provide flexibility to the DSO based on their operating level. CHPs, external suppliers and DR provide their entire flexibility, from their minimum to their maximum level of output power as downward and upward flexibility, respectively.

In contrast, renewable generation (PV and wind) provide upward and downward flexibility according to their bids. The downward bid is equal to the expected operating point dispatched in the energy market, while the upward flexibility is determined through the use of the constant strategy proposed in [26] and implemented in [3] considering the wind and PV data from [40] and [41], respectively. A number of scenarios were generated from the probabilistic forecast data of wind and PV, through the scenario generation process described in [28] with corresponding probability of occurrence. In addition, some of the worst-case scenarios modeled in [3] have been added to the scenario set (with low probability of occurrence) to represent unusual operating system scenarios. The costs associated to upward and downward flexibility of the different type of aggregators; the costs for activation in real-time of both upward and downward flexibility; and the CHP curtailment, renewable spillage and load shedding are shown in Table 2.

4.2. Results

The computations were carried out with CPLEX [42] as a MIP solver on an Intel Xeon E3-1245 3.50 GHz processor with 32 GB RAM. All modelling was performed in the GAMS [43] modelling language.

4.2.1. Base case

Several simulations were carried out for the proposed models considering different numbers of scenarios and risk levels. As a base case, we considered the simulation of both stochastic models for 10 scenarios under a risk level of 5%.

The contracted upward and downward flexibility throughout the day from all available resources, for both the big-M and McCormick approaches, is depicted in Fig. 3. One can see that the McCormick approach requires less flexibility in most periods when compared to the big-M approach. This is because McCormick relaxation is stronger than the big-M relaxation and therefore better approximate the nonlinear behavior of the chance-constraint reformulation.

4.2.2. Sensitivity analysis

For a better understanding of both approaches, a sensitivity analysis was performed. This allow us to validate the applicability of the proposed models under different conditions. These conditions include (*i*) distinct number of scenarios to evaluate the scalability of the solution, and (*ii*) different risk levels of the chance constraint (applied to the active balance equation) to quantify the cost of neglecting unusual operating scenarios that reduce system reliability. Table 3 shows the operating costs and computational performance of each model for 10, 50 and 100 scenarios under the 5% risk level. One can see that the McCormick approach provides solutions with lower expected operating costs than the big-M approach. For 10 scenarios, the McCormick approach is faster than the big-M approach to obtain a solution. As expected, computational effort grows significantly with increasing number of scenarios. However, the McCormick approach generates much more variables than the big-M method, and therefore, with the increasing number of scenarios, loses the advantage of better computational performance. In fact, for 100 scenarios, the McCormick approach requires almost twice the computational time of the big-M approach.

Nevertheless, Table 4 shows the trade-off between the operating cost and system reliability for 10 scenarios. That is, the operating cost that the DSO can save, taking the risk of neglecting unusual operating scenarios (reducing system reliability). For instance, taking a 20% risk level, the DSO is assuming that 2 in 10 scenarios can be ignored. This means that less upward and downward flexibility need to be reserved at first-stage, since the two worst-case scenarios can be ignored, hence reducing operating costs. However, the solution is not as reliable as those that consider a lower risk level, since the optimal solution does not cover all scenarios and therefore the full distribution of uncertainty. Following the most drastic risk level for the big-M approach, DSO reduces system reliability by 20%, with an improvement of about 20% in the operating costs. In parallel, the McCormick approach gets an improvement of about 8% in the operating costs reducing system reliability by 20%.

Moreover, these results show that the McCormick approach provides closer solutions under the different conditions when compared to the big-M approach.

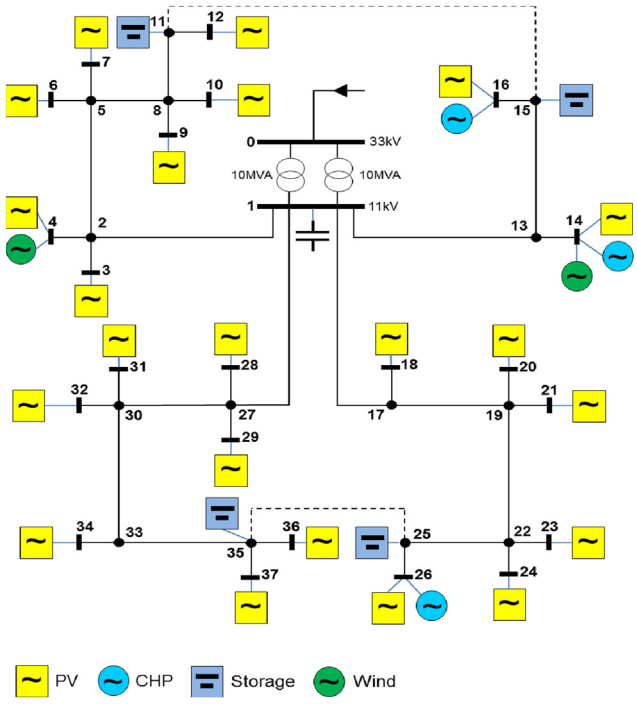

Fig. 2. 37-Bus distribution network [3].

Table 1
DER characteristics and operating point.

DER	Number of units	Total installed power	Operating point P^{op} (MW)		
			Max	*Mean*	*Min*
CHP	3	2.5 (Mva)	1.5	1.15	1
External supplier	1	20 (Mva)	–	–	–
PV	22	7.74 (MWp)	5.55	1.96	0
Wind	2	2.5 (MW)	1.88	1.77	1.52
DR	22	4.65 (MW)	0.1	0.03	0

An overview of the simulation considering both methods for different number of scenarios under different risk levels is depicted in Fig. 4. Fig. 4(a) shows the computational effort of the big-M approach accounting for different risk levels and scenarios number. Fig. 4(b) represents operating costs under different numbers of scenarios and risk levels for the big-M approach. Similarly, Fig. 4(c) and (d) depict the computational effort and operating costs, depending on the scenarios number and risk level for the McCormick approach, respectively. One can see that McCormick approach presents better operating costs than the big-M approach for most simulations, regardless of the number of scenarios and risk level. However, the computational performance through McCormick approach shows a different behavior. As the scenarios increase, the computational performance changes significantly. In fact, the big-M approach performs better McCormick's approach to a high number of scenarios with low risk level. In contrast, for a high number of scenarios and risk level, McCormick approach provides better computational performance than the big-M approach.

5. Conclusions

This work proposes a full linear approach to the predictive distribution management problem (or operational planning of flexibility activation) of the DSO. The DSO can contract power flexibility of DERs in advance of a potential congestion and voltage problem that may arise in the grid. The results show that this approach can provide savings to the DSO, by accounting for the uncertain production of RES in the distribution grid. In addition, results show that distinct convexifications of the nonlinearities have an impact on the solution and computational performance. An important conclusion of this work is that the proposed method shows a preventive behavior when contracting flexibility to cover congestion and voltage problems, accounting for the uncertainty and variability of RES generation. Thus, the chance-constrained solutions enables the DSO to have a trade-off between operating cost and reliability.

Nevertheless, this study points out several directions for future work. One the one hand, the computational performance can be improved by using (*i*) decomposition techniques to decompose the problem into multiple sub-problems, (*ii*) iterative approaches and (*iii*) meta-heuristics. On the other hand, the approximation to the natural behavior of the distribution system can be improved using different convexification techniques of the AC OPF. In addition, different chance-constrained programming approaches can be studied to better assist the decision-maker in assessing the trade-off between operational costs and system reliability.

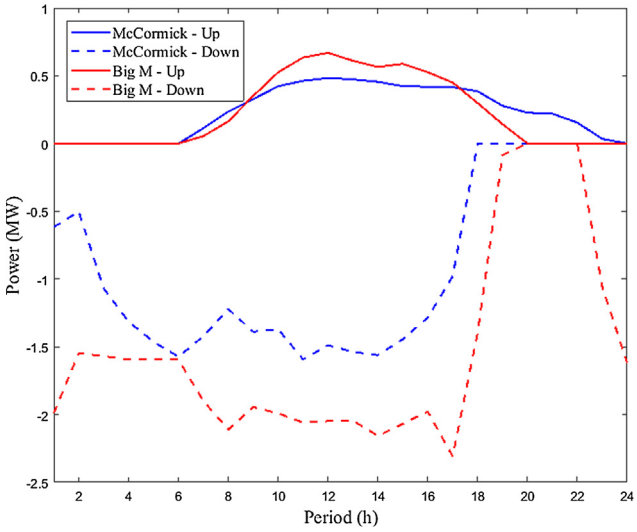

Fig. 3. Contracted flexibility by the DSO under McCormick and big-M approaches.

Table 3
Operating costs and computational performance with varied scenario sizes (risk level of 5% - ε = 0.05).

Scenario number	Big-M		McCormick	
	Time (s)	O.C. (m.u.)	Time (s)	O.C. (m.u.)
10	300	1.246	227	0.877
50	4970	1.224	8955	0.842
100	7781	1.214	14,208	0.825

Table 4
Operating costs and computational performance under different risk levels (scenario number: 10).

Risk level	Big-M		McCormick	
	Time (s)	O.C. (m.u.)	Time (s)	O.C. (m.u.)
5%	300	1.246	227	0.877
10%	3678	1.216	3681	0.816
20%	3682	0.992	3680	0.800

Acknowledgements

This work is supported by the ERDF – European Regional Development Fund through the Operational Programme for Competitiveness and Internationalisation - COMPETE 2020 Programme, and by National Funds through the Portuguese funding agency, FCT - Fundação para a Ciência e a Tecnologia, within project ESGRIDS - Desenvolvimento Sustentável da Rede Elétrica Inteligente/ SAICTPAC/0004/2015- POCI-01-0145-FEDER-016434.

Table 2
Costs of flexibility, activation and spillage for DER.

DER	Upward cost C^{up}(m.u./kWh)	Downward cost C^{dw}(m.u./kWh)	Activation cost C^{act} (m.u./kWh)	Curtailment C^{cut}/spillage C^{spill}/load shedding C_L^{shed} (m.u./kWh)
CHP	0.10	0.06	0.18	0.36
PV	0.11	0.06	0.13	0.30
Wind	0.10	0.05	0.12	0.30
DR – load	0.22	0.17	0.26	0.90

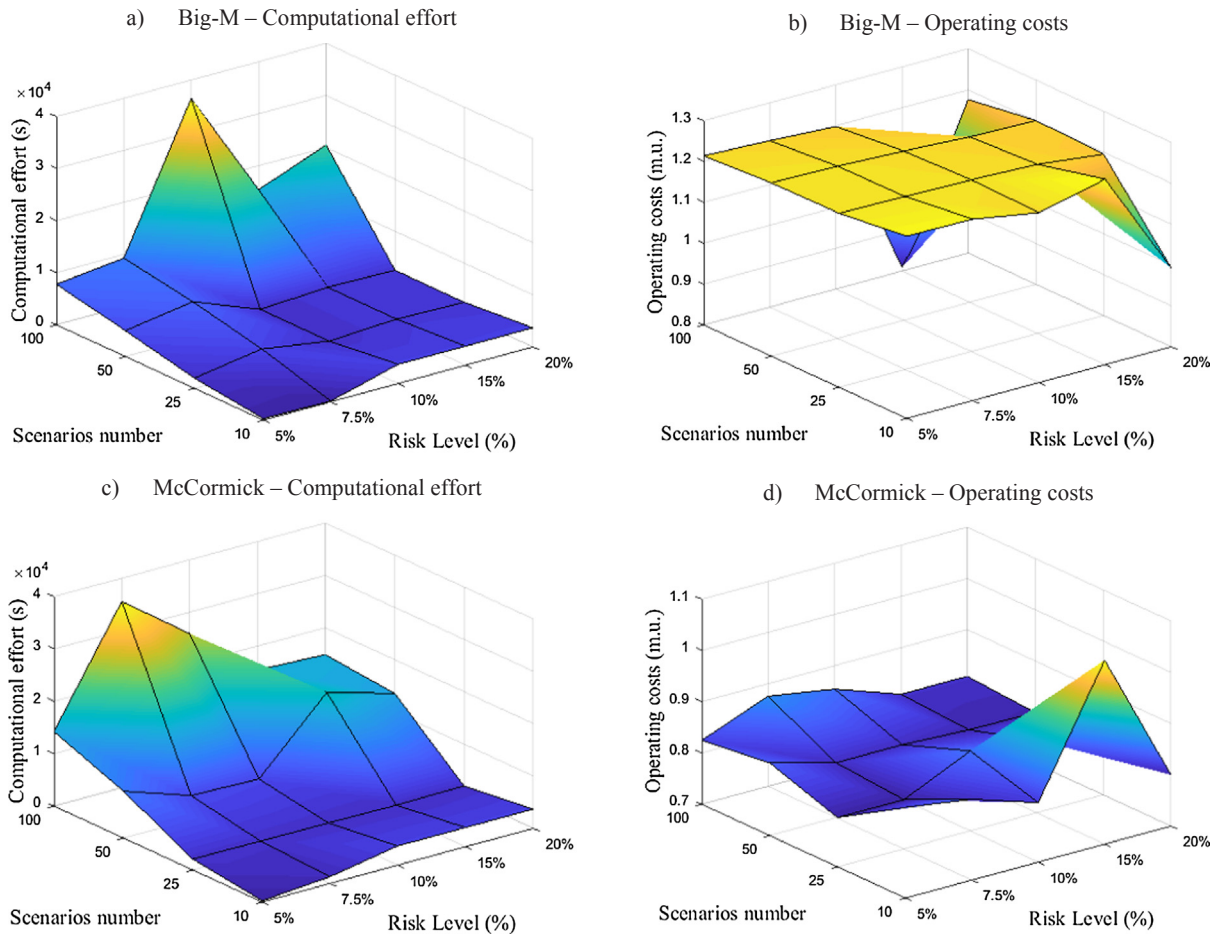

Fig. 4. Risk level vs scenarios number for big M and McCormick approaches considering computational effort and operating costs.

Appendix A. Supplementary material

Supplementary data to this article can be found online at https://doi.org/10.1016/j.ijepes.2019.02.002.

References

[1] Pérez-Arriaga IJ, Ruester S, Schwenen S, Battle C, Glachant J-M. From distribution networks to smart distribution systems: rethinking the regulation of european electricity DSOs. THINK Proj 2013:1–88. doi:10.2870/78510.

[2] Eurelectric. Active distribution system management: a key tool for the smooth integration of distributed generation. Eurelectric 2013:1–53. http://www.eurelectric.org/media/74356/asm_full_report_discussion_paper_final-2013-030-0117-01-e.pdf.

[3] Soares T, Bessa RJ, Pinson P, Morais H. Active distribution grid management based on robust AC optimal power flow. IEEE Trans Smart Grid 2018;9:6229–41. https://doi.org/10.1109/TSG.2017.2707065.

[4] Karagiannopoulos S, Roald L, Aristidou P, Hug G. Operational planning of active distribution grids under uncertainty. In: 10th bulk power syst. dyn. control symp. – IREP; 2017.

[5] Bazrafshan M, Gatsis N. Decentralized stochastic optimal power flow in radial networks with distributed generation. IEEE Trans Smart Grid 2017;8:787–801. https://doi.org/10.1109/TSG.2016.2518644.

[6] Zakariazadeh A, Jadid S, Siano P. Stochastic multi-objective operational planning of smart distribution systems considering demand response programs. Electr Power Syst Res 2014;111:156–68. https://doi.org/10.1016/j.epsr.2014.02.021.

[7] Agalgaonkar YP, Pal BC, Jabr RA. Stochastic distribution system operation considering voltage regulation risks in the presence of PV generation. IEEE Trans Sustain Energy 2015;6:1315–24. https://doi.org/10.1109/TSTE.2015.2433794.

[8] Ul Nazir F, Pal BC, Jabr RA. A two-stage chance constrained volt/var control scheme for active distribution networks with nodal power uncertainties. IEEE Trans Power Syst 2018:1–11. https://doi.org/10.1109/TPWRS.2018.2859759.

[9] Cao Y, Tan Y, Li C, Rehtanz C. Chance-constrained optimization-based unbalanced optimal power flow for radial distribution networks. IEEE Trans Power Deliv 2013;28:1855–64. https://doi.org/10.1109/TPWRD.2013.2259509.

[10] Saunders CS. Point estimate method addressing correlated wind power for probabilistic optimal power flow. IEEE Trans Power Syst 2014;29:1045–54. https://doi.org/10.1109/TPWRS.2013.2288701.

[11] Jabr RA. Adjustable robust OPF with renewable energy sources. IEEE Trans Power Syst 2013;28:4742–51. https://doi.org/10.1109/TPWRS.2013.2275013.

[12] Zhang Y, Giannakis GB. Robust optimal power flow with wind integration using conditional value-at-risk. IEEE Int Conf Smart Grid Commun 2013:654–9. https://doi.org/10.1109/SmartGridComm.2013.6688033.

[13] Bai X, Qu L, Qiao W. Robust AC optimal power flow for power networks with wind power generation. IEEE Trans Power Syst 2016;31:4163–4. https://doi.org/10.1109/TPWRS.2015.2493778.

[14] Ozturk UA, Mazumdar M, Norman BA. A solution to the stochastic unit commitment problem using chance constrained programming. IEEE Trans Power Syst 2004;19:1589–98. https://doi.org/10.1109/TPWRS.2004.831651.

[15] Pozo D, Contreras J. A chance-constrained unit commitment with an n-k security criterion and significant wind generation. IEEE Trans Power Syst 2013;28:2842–51. https://doi.org/10.1109/TPWRS.2012.2227841.

[16] Wu H, Shahidehpour M, Li Z, Tian W. Chance-constrained day-ahead scheduling in stochastic power system operation. IEEE Trans Power Syst 2014;29:1583–91. https://doi.org/10.1109/TPWRS.2013.2296438.

[17] Zhang H, Li P. Chance constrained programming for optimal power flow under uncertainty. IEEE Trans Power Syst 2011;26:2417–24. https://doi.org/10.1109/TPWRS.2011.2154367.

[18] Wu L, Shahidehpour M, Li T. Stochastic security-constrained unit commitment. IEEE Trans Power Syst 2007;22:800–11. https://doi.org/10.1109/TPWRS.2007.894843.

[19] Zheng QP, Wang J, Liu AL. Stochastic optimization for unit commitment - A review. IEEE Trans Power Syst 2015;30:1913–24. https://doi.org/10.1109/TPWRS.2014.2355204.

[20] Bienstock D, Chertkov M, Harnett S. Chance constrained optimal power flow: risk-aware network control under uncertainty. SIAM Rev 2014;56:461–95. https://doi.org/10.1137/130910312.

[21] Wang Q, Guan Y, Wang J. A chance-constrained two-stage stochastic program for unit commitment with uncertain wind power output. IEEE Trans Power Syst 2012;27:206–15. https://doi.org/10.1109/TPWRS.2011.2159522.

[22] Zhao C, Wang Q, Wang J, Guan Y. Expected value and chance constrained stochastic unit commitment ensuring wind power utilization. IEEE Trans Power Syst 2014;29:2696–705. https://doi.org/10.1109/TPWRS.2014.2319260.

[23] Ulian A, Sebastian M, Bartolucci G, Gutshi C. Business use cases definition and requirements. Deliv D21, EU Proj EvolvDSO 2014:1–226. http://www.evolvdso.eu/

Home/Results.
[24] Chrysochos AI, Kryonidis GC, Kontis EO, Demoulias CS, Papagiannis GK. Dynamic equivalent models for the simulation of controlled DRES. Deliv D 2014:1–70. http://www.project-increase.eu/index.php?cmd=s&id=74.
[25] Madureira A, Bessa R, Meirinhos J, Fayzur D, Filipe J, Messias AA, et al. The impact of solar power forecast errors on voltage control in smart distribution grids. In: 23rd int. conf. electr. distrib. (CIRED 2015), Lyon, Fr.; 2015.
[26] Soares T, Pinson P, Jensen TV, Morais H. Optimal offering strategies for wind power in energy and primary reserve markets. IEEE Trans Sustain Energy 2016;7:1–10. https://doi.org/10.1109/TSTE.2016.2516767.
[27] Coffrin C, Van Hentenryck P. A linear-programming approximation of AC power flows. INFORMS J Comput 2014;26:718–34. https://doi.org/10.1287/ijoc.2014.0594.
[28] Pinson P, Madsen H, Nielsen HA, Papaefthymiou G, Klöckl B. From probabilistic forecasts to statistical scenarios of short-term wind power production. Wind Energy 2009;12:51–62. https://doi.org/10.1002/we.284.
[29] Gröwe-Kuska N, Heitsch H, Römisch W. Scenario reduction and scenario tree construction for power management problems. In: 2003 IEEE bol. powertech - conf. proc., Bologna, Italy; 2003. doi:10.1109/PTC.2003.1304379.
[30] Michalke G, Hansen AD. Grid support capabilities of wind turbines. Handb. Wind Power Syst. Springer; 2014. p. 569–90. doi:10.1007/978-3-642-41080-2.
[31] Haghighat H, Kennedy SW. A model for reactive power pricing and dispatch of distributed generation. IEEE PES Gen. Meet. Minneapolis, US; 2010. p. 1–10. doi:10.1109/PES.2010.5589576.
[32] ERSE. Despacho no 7253/2010. Diário Da República [in Port 2010;2:21945–9. http://www.erse.pt/pt/legislacao/Legislacao/Attachments/1411/Despacho 7253_2010.pdf.
[33] Venzke A, Halilbasic L, Markovic U, Hug G, Chatzivasileiadis S. Convex relaxations of chance constrained AC optimal power flow. IEEE Trans Power Syst 2018;33:2829–41. https://doi.org/10.1109/TPWRS.2017.2760699.
[34] Zhang Y, Wang J, Zeng B, Hu Z. Chance-constrained two-stage unit commitment under uncertain load and wind power output using bilinear benders decomposition. IEEE Trans Power Syst 2017;32:3637–47. https://doi.org/10.1109/TPWRS.2017.2655078.
[35] Zeng B, An Y, Kuznia L. Chance constrained mixed integer program : bilinear and linear formulations, and benders decomposition. Math - Optim Control 2014:1–30.
[36] Ackooij W van, Zorgati R, Henrion R, Möller A. Chance constrained programming and its applications to energy management. In: Dritsas I, editor. Stoch. optim. - seeing optim. uncertain 1st ed.Rijeka: InTech; 2011. p. 32. https://doi.org/10.5772/15438.
[37] Mohagheghi E, Geletu A, Bremser N, Alramlawi M, Gabash A, Li P. Chance constrained optimal power flow using the inner-outer approximation approach. Optim Control 2018:6.
[38] McCormick GP. Computability of global solutions to factorable nonconvex programs: Part I - Convex underestimating problems. Math Program 1976;10:147–75. https://doi.org/10.1007/BF01580665.
[39] Gass SI. Linear programming. Encyclopedia of statistical sciences Wiley; 2006. https://doi.org/10.1002/0471667196.ess1466.pub2.
[40] Bukhsh WA, Zhang C, Pinson P. Data for stochastic multiperiod opf problems n.d. https://sites.google.com/site/datasmopf/.
[41] Bessa RJ, Trindade A, Miranda V. Spatial-temporal solar power forecasting for smart grids. IEEE Trans Ind Informatics 2015;11:232–41. https://doi.org/10.1109/TII.2014.2365703.
[42] IBM. CPLEX optimizer 12.0 - user's manual. n.d.
[43] Rosenthal R. GAMS – a user's guide. Washington, DC: GAMS Development Corporation; 2008.